RSC Advances

ROYAL SOCIETY OF CHEMISTRY

www.rsc.org/advances

Cite this: DOI: 10.1039/c0xx00000x

www.rsc.org/xxxxxx

ARTICLE TYPE

Bio-inspired synthesis of carbon hollow microspheres from *Aspergillus flavus* conidia for lithium-ion batteries

Sangui Liu, [#a,b] Cuiping Mao, [#a,b] Ling Wang [a,b], Min Jia [a,b], Qiangqiang Sun [a,b], Yang Liu,[c] Maowen Xu,* [a,b] and Zhisong Lu* [a,b]

Received (in XXX, XXX) Xth XXXXXXXXX 20XX, Accepted Xth XXXXXXXXX 20XX
DOI: 10.1039/b000000x

A conidium-templated approach is developed to prepare carbon hollow microspheres, which demonstrate great potentials to be applied as anode materials in lithium-ion batteries. This work may provide a novel method to fabricate conidium-derived carbon materials for energy systems.

Carbon is an old but new material. It has been more than 3,000 years since the first carbon material, carbon black, was used as ink, pigment, and tattoos[1]. Motivated by rapid advances of nanotechnology, lots of carbon materials with unique or greatly improved properties, such as graphitic oxide[2], fullerenes[3], carbon nanotubes[4] and graphene[5], have been continuously discovered in the past few decades. The emergence of those materials significantly accelerates the development of major industries such as electronics, aerospace and new energy systems. Fabrication of carbon materials with designed structures has become one of the hottest research topics in material sciences.

Among various structured carbon materials, the ones with hollow spherical morphologies have attracted considerable interests. Due to their high packing density, large specific surface area and maximal structure stability, hollow carbon spheres have already been utilized for varieties of applications including sensors, adsorbents, catalytic supports and energy storage[6-14]. Hollow carbon spheres are also suggested to be promising anode materials for lithium ion batteries (LIBs) because they possess a large reaction interface and short diffusion length to facilitate Li^+ transport, as well as sufficient space to buffer the volume change in Li^+ insertion and extraction processes[15,16]. So far, hydrothermal approaches[9, 11] and hard/soft template-mediated synthesis[12, 14, 17, 18] are the most widely employed methods for the preparation of hollow carbon spheres. Although spherical structure with an excellent hollow interior could be efficiently produced, the involvement of high pressure in the synthesis and the tedious procedures for the preparation and removal of templates greatly hinder their broad applications.

Aspergillus flavus (*A. flavus*) is a fungus that grows by producing thread like branching mycelia. During its asexual reproduction, mycelia produce specialized stalks called conidiophore, on which conidia are borne. Conidium is a single cell with smooth surface and sphere or oval shape, which has the capability to develop into a new individual[19, 20]. Inspired by the state of the arts that use biomass as carbon sources to produce carbon materials, it may be possible to fabricate carbon materials with hollow and spherical morphologies using conidia as bio-templates. However, to the best of our knowledge, fabrication of conidia-derived hollow carbon spheres has never been reported to date.

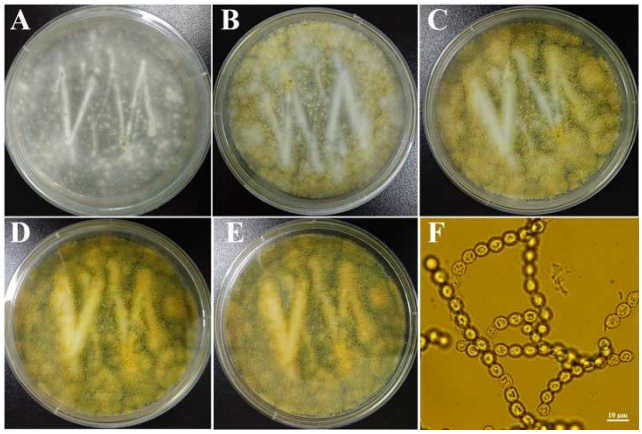

Fig. 1 Appearance of the growth of *A. flavus* on the (A) 1st day, (B) 3rd day, (C) 5th day , (D) 7th day and (E) 9th day; (F) Optical micrograph of *A. flavus* conidia on the 7th day.

Herein, for the first time, we develop a facile and efficient method to prepare *A. flavus* conidium-derived hollow carbon spheres, which are doped by nitrogen (*N*), phosphorus (*P*) and sulphur (*S*), as anode materials for LIBs. *A. flavus* kindly provided by Institute of Agro-Products Processing Science and Technology, Chinese Academy of Agricultural Sciences was inoculated on a potato dextrose agar (PDA) medium and cultured at 30 °C for the growth of conidia[21]. After 1 day of incubation, many white colonies can be found on the agar plates (Fig. 1A). Optical micrograph clearly shows the branched filaments of those white substances (Fig. S1A), confirming the growth of branching mycelia on the agar plates. On the 3rd day the colour of some colonies changes from white to yellow, which is the indicator for the formation of conidia (Fig. 1B). As the time elongates from 3 to 7 days, more yellow colonies are observed and the colour of the conidia becomes brown, showing the large amount production and mature of conidia (Fig. 1C and 1D). The optical micrographs display a typical conidiophore structure on day 3, the well-dispersed conidia on day 5 and the aggregation of conidia on day

7 (Fig. S1B-S1D), respectively. No significant alteration of the colonies occurs on day 9 (Fig. 1E). Based on the findings, we harvest conidia on the 7th day to obtain high quality bio-templates. As being illustrated in Fig. 1F, the conidia possess spherical morphologies with the size range from 3.5 to 5 μm.

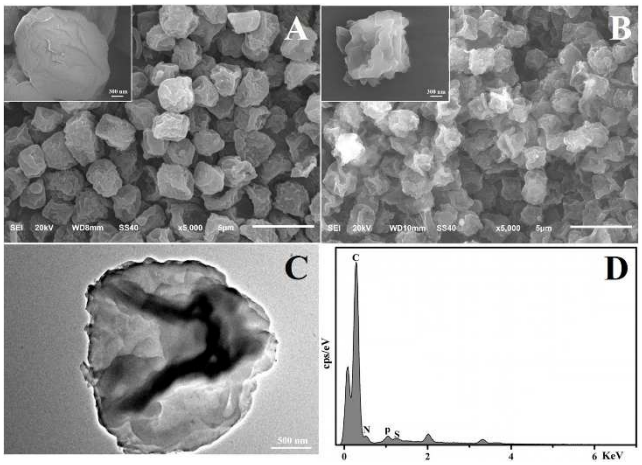

Fig. 2 SEM images of conidia before (A) and after calcination (B) (insets: corresponding magnified SEM images of single conidium); (C) TEM image and (D) EDX spectrum of conidia after calcination.

In order to maintain the spherical structures of the conidia, fixation and dehydration procedures were carried out in the present work. After above treatment, the conidia show an oval shape with some sulcus and wrinkles on the surface (Fig. 2A). The size of the treated conidia ranges from 1 to 3 μm, which is smaller than that observed in Fig. 1F. The dehydration may cause the surface folding and size reduction of the products. Comparatively, obvious alterations in conidium characteristics are exhibited after calcination (Fig. 2B). Conidia are shrunken and more wrinkles appear on the microsphere surface. TEM image clearly shows the same morphologies and the hollow interior of the calcinated conidium (Fig. 2C). Since water is the main component of a conidium, the removal of water during the dehydration and calcination processes leaves the empty internal space in the microspheres. Pyrolytic reactions occurred in the heat treatment process may also lead to the weight loss and partially collapsing of the microspheres. The main peak of carbon in energy-dispersive X-ray (EDX) spectrum verifies the carbon nature of the prepared hollow microspheres (Fig. 2D). The containing of *N*, *P* and *S* in the conidia causes the three weak peaks, suggesting the doping of *N*, *P* and *S* in the synthesized hollow carbon spheres. The result is consistent with the XPS spectra in Fig. S3. The absence of oxygen in the sample proves the thorough calcination of the bio-templates. It is confirmed that conidium-derived carbon microspheres with hollow structures are synthesized via the successive fixation, dehydration and calcination steps.

Fourier transform infrared spectroscopy (FTIR) and Raman spectroscopy were conducted to analyse surface chemical groups of the samples. FTIR spectrum of conidia has many adsorption peaks, which can be assigned to the surface functional groups of the bio-templates such as C=O, C–O, C–H, and –O–H. All the absorption peaks disappear after calcination (Fig. 3A). The phenomenon is due to the removal of chemical groups during the

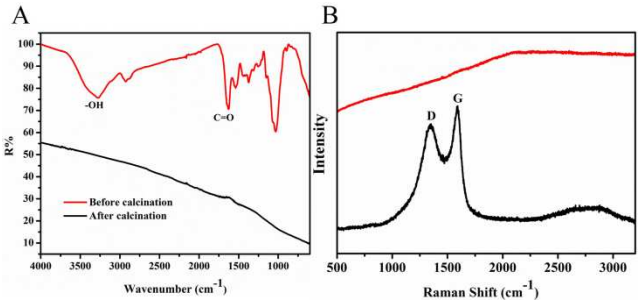

Fig. 3 (A) FTIR and (B) Raman spectra of the *A. flavus* conidia before (red) and after calcination (black).

calcination. The X-ray diffraction pattern of conidia displays one peak at around 19.8°, which may be attributed to the cellulose, the major component of the extracellular coat surrounding conidia[22]. The heat-treated samples have two obvious broad peaks located at 23.5° and 43.4°, corresponding to the (002) and (100) planes of graphite respectively (Fig. S4). The data suggest the partial graphitization of conidia, which is further confirmed by Raman spectroscopy. In comparison to the featureless spectrum of the untreated conidia, two peaks at 1345 (D band) and 1588 cm^{-1} (G band), attributed to defected carbon crystallites and crystalline graphite, are exhibited in Raman spectrum of calcinated samples (Fig. 3B). Above results strongly verify the efficient carbonization of the conidia samples in the calcination process. Before applying the conidium-derived hollow carbon spheres in LIBs, the Brunauer–Emmett–Teller (BET) specific surface area and porosity were studied with nitrogen adsorption–desorption analysis (Fig. S5). The BET specific surface area of the materials is 309.9 m^2 g^{-1}, while mesopores with the size less than 10 nm are calculated according to the adsorption branches.

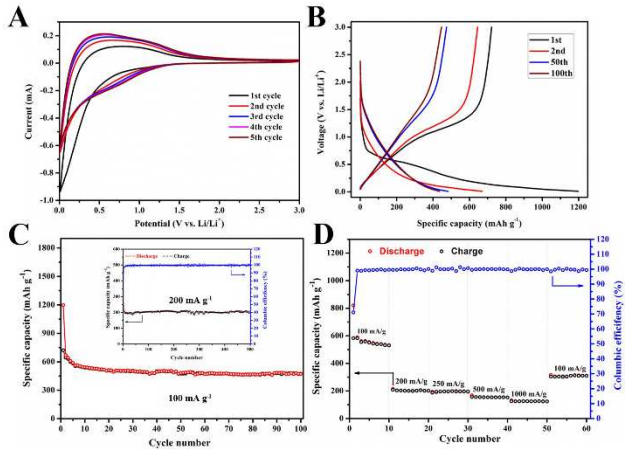

Fig. 4 (A) Cyclic voltammogram curves at a scan rate of 0.5 mV s^{-1}; (B) Charge-discharge curves at current density of 100 mA g^{-1}; (C) Cycling performance at 100 mA g^{-1} for 100 cycles (inset: cycling performance and coulombic efficiency at 200 mA g^{-1} for 500 cycles); (D) Capacity and coulombic efficiency over cycling at different rates.

The calcinated *A. flavus* conidia materials were further investigated as anode material for LIBs. The electrochemical performance is revealed in Fig. 4. As show in Fig. 4A, the initial five consecutive cyclic voltammograms (CVs) are scanned continuously between 0.01 and 3.0 V at scan rate of 0.5 mV s^{-1}. Fig. 4B shows the charge–discharge profiles of the carbonaceous

conidia anode at a current density of 100 mA g^{-1}. In the first cycle, a plateau at 0.5-0.75 V appears following the rapid voltage drop, which is probably due to the formation of solid electrolyte interphase (SEI) and other side reactions[23]. The initial discharge capacity is as high as 1198 mAh g^{-1} and the reversible capacity of the second cycle is 685 mAh g^{-1}. The initial irreversible capacity is an unavoidable phenomenon in carbonaceous electrodes in LIB, which may be ascribed to reduction of the electrolyte, the formation of SEI layer, and/or irreversible lithium insertion into special positions in the vicinity of residual H atoms in the carbon material[24]. The cycle performance was evaluated at current density of 100 mA g^{-1} and 200 mA g^{-1}, respectively. As shown in Fig. 3C, the calcinated conidia anode exhibits extraordinary cycling stability both at 100 and 200 mA g^{-1}. It is worthy to note that the reversible capacity is still 475 mAh g^{-1} after 100 cycles, which is higher than the theoretical capacity of 372 mAh g^{-1}. This is presumably due to the existence of *N*, *P* and *S* elements, leading to the change of graphite crystalline structure[25, 26]. In addition, large numbers of mesopores with size less than 10 nm may act as reservoirs and paths for Li ions and electrolytes[27, 28]. Furthermore, the large surface area provides sufficient electrode/electrolyte interface and facilitates rapid charge-transfer reaction. Even at a current density of 200 mA g^{-1}, the cell still shows excellent cycling ability with high coulombic efficiency (Fig. 4C inset). After 500 cycles, the morphology of the materials still can be maintained (Fig. S8). Fig. 4D shows the rate performance, which was investigated by cycling the cell at various current densities from 100 to 1000 mA g^{-1}. During first 10 cycles at 100 mA g^{-1}, the discharge capacity gradually decreases and remains a value of 530 mAh g^{-1}. The reversible specific capacities are 205, 195, 154 and 125 mAh g^{-1} at 200, 250, 500 and 1000 mA g^{-1}, respectively. The cell shows an excellent stability at all above current densities.

In summary, we demonstrate a novel bio-templated method to facilely obtain *A. flavus* conidium-derived hollow carbon spheres with large specific surface area for the first time. LIBs with the as-prepared materials as anode exhibits a good discharge/charge capacity, superior cycling stability and excellent coulombic efficiency. This work may not only provide a novel approach for the fabrication of carbon materials with conidia as a bio-template, but also demonstrate their potential capability in the energy systems.

Acknowledgements

This work is financially supported by National Program on Key Basic Research Project of China (973 Program) under contract No.2013CB127800, Chongqing Key Laboratory for Advanced Materials and Technologies of Clean Energies under cstc2011pt-sy90001 and Start-up grant under SWU111071 from Southwest University (Chongqing, China). Z. S. Lu would like to thank the supports by the Specialized Research Fund for the Doctoral Program of Higher Education (RFDP) (Grant No. 20130182120025), Young Core Teacher Program of the Municipal Higher Educational Institution of Chongqing and Chongqing Natural Science Foundation (cstc2012jjA1137).

Notes and references

a Institute for Clean Energy & Advanced Materials, Faculty of Materials and Energy, Southwest University, 1 Tiansheng Road, Chongqing 400715, P. R. China.

b Chongqing Key Laboratory for Advanced Materials & Technologies of Clean Energies, 1 Tiansheng Road, Chongqing 400715, P. R. China. Fax: +86-23-68254969; Tel: +86-23-68254732; E-mail: xumaowen@swu.edu.cn and zslu@swu.edu.cn.

c Institute of Agro-Products Processing Science and Technology, Chinese Academy of Agricultural Sciences/Key Laboratory of Agro-Products Processing, Ministry of Agriculture, No. 2 Yuan Ming Yuan West Road, Beijing 100193, P. R. China.

† Electronic Supplementary Information (ESI) available: [Experimental section]. See DOI: 10.1039/b000000x

1. W. H. Suh, K. S. Suslick, G. D. Stucky and Y.-H. Suh, *Prog. Neurobiol.*, 2009, **87**, 133-170.
2. W. S. Hummers and R. E. Offeman, *J. Am. Chem. Soc.*, 1958, **80**, 1339-1339.
3. H. W. Kroto, J. R. Heath, S. C. O'Brien, R. F. Curl and R. E. Smalley, *Nature*, 1985, **318**, 162-163.
4. S. Iijima, *Nature*, 1991, **354**, 56-58.
5. K. S. Novoselov, A. K. Geim, S. V. Morozov, D. Jiang, Y. Zhang, S. V. Dubonos, I. V. Grigorieva and A. A. Firsov, *Science*, 2004, **306**, 666-669.
6. L. Pan, A. Chortos, G. Yu, Y. Wang, S. Isaacson, R. Allen, Y. Shi, R. Dauskardt and Z. Bao, *Nat. Commun.*, 2014, **5**.
7. J. Zhou, C. Tang, B. Cheng, J. Yu and M. Jaroniec, *ACS Appl.Mater. Interfaces*, 2012, **4**, 2174-2179.
8. P. K. Tripathi, L. Gan, M. Liu, X. Ma, Y. Zhao, D. Zhu, Z. Xu, L. Chen and N. N. Rao, *Mater. Lett.*, 2014, **120**, 108-110.
9. S. P. Dubey, A. D. Dwivedi, I.-C. Kim, M. Sillanpaa, Y.-N. Kwon and C. Lee, *Chem. Engin. J*, 2014, **244**, 160-167.
10. J. Wu, C. Jin, Z. Yang, J. Tian and R. Yang, *Carbon*, 2015, **82**, 562-571.
11. Y. Han, X. Dong, C. Zhang and S. Liu, *J. Power Sources*, 2012, **211**, 92-96.
12. X. Fang, J. Zang, X. Wang, M.-S. Zheng and N. Zheng, *J. Mater. Chem. A*, 2014, **2**, 6191-6197.
13. D. Cai, L. Ding, S. Wang, Z. Li, M. Zhu and H. Wang, *Electrochim. Acta*, 2014, **139**, 96-103.
14. F. Böttger-Hiller, P. Kempe, G. Cox, A. Panchenko, N. Janssen, A. Petzold, T. Thurn-Albrecht, L. Borchardt, M. Rose, S. Kaskel, C. Georgi, H. Lang and S. Spange, *Angew. Chem. Int. Ed.*, 2013, **52**, 6088-6091.
15. Y. Wang, F. Su, J. Y. Lee and X. S. Zhao, *Chem. Mater.*, 2006, **18**, 1347-1353.
16. K. T. Lee, J. C. Lytle, N. S. Ergang, S. M. Oh and A. Stein, *Adv. Funct. Mater.*, 2005, **15**, 547-556.
17. X. Liu, L. Zhou, Y. Zhao, L. Bian, X. Feng and Q. Pu, *ACS Appl. Mater. Interfaces*, 2013, **5**, 10280-10287.
18. J. Han, G. Xu, B. Ding, J. Pan, H. Dou and D. R. MacFarlane, *J. Mater. Chem. A*, 2014, 2, 5352-5357.
19. C. Y. Kohiyama, M. M. Yamamoto Ribeiro, S. A. G. Mossini, E. Bando, N. d. S. Bomfim, S. B. Nerilo, G. H. O. Rocha, R. Grespan, J. M. G. Mikcha and M. Machinski Jr, *Food Chem.*, 2015, **173**, 1006-1010.
20. M. T. Hedayati, A. C. Pasqualotto, P. A. Warn, P. Bowyer and D. W. Denning, *Microbiology*, 2007, **153**, 1677-1692.
21. C.-S. Zhang, F.-G. Xing, J. N. Selvaraj, Q.-L. Yang, L. Zhou, Y.-J. Zhao and Y. Liu, *Biochem. Syst. Ecol.*, 2013, **50**, 147-153.
22. P. Zhang, A. C. McGlynn, C. M. West, W. F. Loomis and R. L. Blanton, *Differentiation*, 2001, **67**, 72-79.
23. Z. Liu, X. Zhang, S. Poyraz, S. P. Surwade and S. K. Manohar, *J. Am. Chem. Soc.*, 2010, **132**, 13158-13159.
24. L. Wang, Z. Schnepp and M. M. Titirici, *J. Mater. Chemistry A*, 2013, **1**, 5269-5273.
25. S. T. Mayer, R. W. Pekala, R. L. Morrison and J. L. Kaschmitter, Google Patents, 1994.
26. Y. P. Wu, S. Fang, Y. Jiang and R. Holze, *J. Power Sources*, 2002, **108**, 245-249.

27. L. Chen, Y. Zhang, C. Lin, W. Yang, Y. Meng, Y. Guo, M. Li and D. Xiao, *J. Mater. Chem. A*, 2014, **2**, 9684-9690.
28. N. A. Kaskhedikar and J. Maier, *Adv. Mater.*, 2009, **21**, 2664-2680.

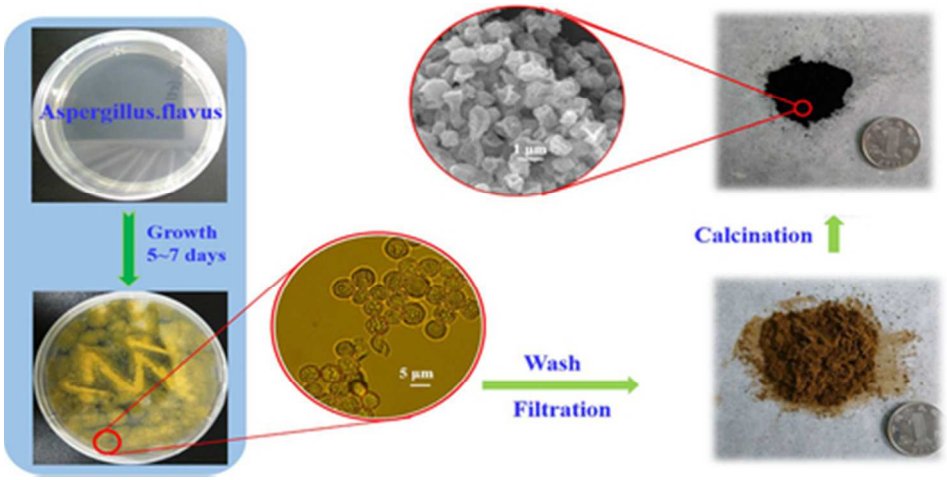

39x19mm (300 x 300 DPI)